ELSEVIER

Computers in Biology and Medicine 36 (2006) 1336–1350

Computers in Biology and Medicine

www.intl.elsevierhealth.com/journals/cobm

A numerical coupling model to analyze the blood flow, temperature, and oxygen transport in human breast tumor under laser irradiation

Ying He[a,*], Minoru Shirazaki[b], Hao Liu[c], Ryutaro Himeno[a], Zhigang Sun[d]

[a] *Computational Biomechanics Unit, RIKEN, 2-1 Hirosawa, Wako-shi 351-0198, Japan*
[b] *Faculty of Education and Human Sciences, Yokohama National University, 79-1 Tokiwadai, Hodogaya-ku, Yokohama 240-8501, Japan*
[c] *Faculty of Engineering, Chiba University, 1-33 Yayoi-cho, Inage-ku, Chiba 263-8522, Japan*
[d] *ASTOM R & D, RIKEN, 2-1 Hirosawa, Wako-shi 351-0198, Japan*

Received 9 March 2005; accepted 5 August 2005

Abstract

The aim of this study is to investigate the variation of the blood perfusion rate and distribution of oxygen partial pressure (PO_2) in human tumors by a coupling numerical model when laser irradiation is used as an adjuvant method in the treatment of cancer. A two-dimensional finite element (FE) thermal model of a human breast with a tumor was developed. The blood circulation inside the breast was modeled using one-dimensional non-linear equations of pulsatile fluid flow. The distribution of PO_2 inside the capillaries, tumor vessels, and surrounding tissue was obtained by the Krogh analysis model. Finally, the variations of the average tumor temperature, blood perfusion, and PO_2 during laser heating were computed by coupling the blood circulation, FE thermal, and oxygen transport models.

Keywords: Bioheat transfer; Tumor; Laser irradiation; FEM; Blood perfusion; One-dimensional flow model; Oxygen transport; Oxygen partial pressure; Numerical simulation

* Corresponding author. Tel.: +81 48 462 1111x3896; fax: +81 48 467 9610.
E-mail address: heying@riken.jp (Y. He).

0010-4825/$ - see front matter © 2005 Elsevier Ltd. All rights reserved.
doi:10.1016/j.compbiomed.2005.08.004

Nomenclature

A	cross-sectional area of blood vessel, m^2
A_s	surface area of blood vessel per unit length, m
a	absorption coefficient, m^{-1}
b	variation coefficient in Eq. (17), K^{-1}
c	specific heat, J/kg K
E	Young's modulus, kg/s^2 m
h	wall thickness of blood vessel, m
h_{ves}	heat transfer coefficient, W/m^2 K
I	laser beam power intensity, W/m^2
k_p	parameter proportional to the bending stiffness of the tube wall, Pa
n	normal direction
p	pressure, Pa
PO_2	oxygen partial pressure, Pa
q	flow rate, m^3/s
r	r direction in cylindrical coordinate, m
T	temperature, K
t	time, s
x	axial length coordinate, m
z	z direction in cylindrical coordinate, m
δ	thickness of the boundary layer, m
λ	thermal conductivity, W/mK
ν	kinematic viscosity, m^2/s
ρ	density, kg/m^3
ω	blood perfusion rate, $m^3/s/m^3$
ω_{rd}	radial frequency, rad/s

Subscripts

0	initial state
b	blood
e	element
f	fluid
s	surface
t	tissue

1. Introduction

The effect of hyperthermia is not limited to tumor cells but is also observed on the microvasculature. The effect of hyperthermia on tumor vasculature is of considerable interest since controlling the tumor blood flow can improve the efficiency of tumor treatment. For example, in radiotherapy, improving the blood flow can increase the tumor oxygenation; similarly in chemotherapy, increasing the blood flow helps

increase the delivery of appropriate pharmacological agents. On the other hand, vascular insufficiency and poor tumor blood flow are desirable in hyperthermia since the blood flow dissipates energy from the tissues.

The detailed measurement of microvascular flow [1] in the amelanotic melanoma A-Mel-3 of a hamster under hyperthermia was carried out by intravital microscopy, quantitative video image analysis, and a transparent chamber technique. It was observed that when the heating temperature in the melanoma did not exceed 40 °C, the tumor blood flow increased. However, when the heating temperature exceeded 42 °C and lasted for at least 15 min, the diameters of the arterioles feeding the tumor became constricted and the tumor blood flow decreased.

The spatial distribution of blood flow in the normal porcine skeletal muscle before, during, and after a period of regional microwave hyperthermia was examined by the radioactive microsphere method [2]. It was found that although the blood flow in muscles might be considered to be uniform prior to heating, regional heating could generate a non-uniform flow distribution, which was a function of the tissue temperature distribution. Further, the blood flow was greater in those tissue samples in which higher tissue temperatures were recorded and lesser in those samples further from the applicators' peak specific absorption rate (SAR).

The relationship between the changes in oxygen partial pressure (PO_2) and blood flow in heated tumors was investigated by animal experiments [3]. The result showed that tumor oxygenation or PO_2 increases immediately after mild temperature hyperthermia. In another study by Song and coworkers [4] the damage caused to a tumor when an antitumor drug was used alone and when it was used in combination with hyperthermia was investigated, and it was observed that there was a longer growth delay when an antitumor drug was used in combination with mild hyperthermia.

In summary, exploring the hyperthermia-blood flow-oxygenation relationship is crucial for the realization of targeted drug delivery. Modeling the hyperthermia-blood flow-tissue interaction may be beneficial for the analysis and optimization of the parameters governing planned hyperthermia treatment procedures.

Several modeling studies have been conducted to illustrate the effect of variation of blood flow rate under local heating. Shulman et al. [5] modeled the blood perfusion variation under local hyperthermia treatment conditions using a function of temperature and the dimensionless "physiological" time. The blood flow rate (BFR) function and the one-dimensional bioheat transfer equation were numerically solved to describe different heat transfer processes that occur during the clinical treatment; therefore, the temperature and the blood flow rate could be monitored simultaneously.

Guiot et al. [6] investigated the blood perfusion and thermal response of a tissue during hyperthermia in recurrent breast cancer. They numerically evaluated the "effective conductivity" (k_{eff}) of the perfused tissue by fitting the measured temperatures to the computed ones. They found that the values of effective conductivity for different patients varied due to different blood perfusion rates. Therefore, they believe that a "perfusion map" and a "temperature map" should be monitored within the heated volume throughout the hyperthermia session.

On the other hand, some researchers are of the opinion that heat transfer in the tissue and blood vessels should be considered separately using the energy equations in tissue and blood vessels [7,8], instead of using heat transfer coefficients. These researchers directly simulated the temperature distribution inside blood vessels and tissue.

A common feature of the above-mentioned modeling studies is that they intend to capture the variation of blood flow rate with temperature without considering the effects of blood pressure and vessel characteristics. As regards the determinants of tumor blood flow, Jain [9] in his review suggested that

a knowledge of the response of the pressure difference between the arterial and venuous ends of tissue circulation, the blood viscosity, and the geometrical resistance (hindrance) to various chemical stimuli and physical stimuli (radiation, heat, photodynamics therapy, hemodilation) may be the key issue that required investigation.

The purpose of this study is to numerically investigate the response of blood flow and oxygen diffusion to the laser irradiation in a human breast tumor. First, a two-dimensional finite element (FE) thermal model is developed to simulate the absorption of laser energy. Next, the one-dimensional model of fluid flow in elastic tubes is used to model the blood flow in the vessel network with neoplastic vasculature. Subsequently, PO_2 distribution is analyzed in normal and tumor tissue units through the Krogh model [10]. These models were weakly coupled by data transfer; thus, the variation of blood flow and oxygen distribution under laser radiation can be obtained.

2. The breast model under laser irradiation

Fig. 1(a) shows a schematic diagram of a laser-irradiated breast and the solution domain. The breast model is assumed to be hemispherical in shape with a subcutaneous fat layer and gland regions. A 10-mm diameter tumor is located 6 mm beneath the surface with its center on the z-axis. The geometrical data are obtained from the study of Ng and Sudharsan [11]. The laser beam strikes the tissue from a distance. At the skin surface, there is a water bolus to keep the temperature low.

The tumor vessels are different from the vessels in normal tissues, which are permeable, fragile, and larger. Less et al. [12] found that the mean values of the diameter and the length of capillaries in a mammary adenocarcinoma are 10 and 67 μm, respectively [12]. On the other hand, the mean values of diameter and the length of capillaries in normal tissues are 5 and 500 μm, respectively. The tumor vascular beds are considered to form from the vascular beds in the normal tissues, which are parallel, in series, or in a combination type [13]. Fig. 1b shows the modeled blood vessel network in a breast tumor. Here, we consider that the tumor vascular beds are parallel to the normal vascular beds. The geometrical

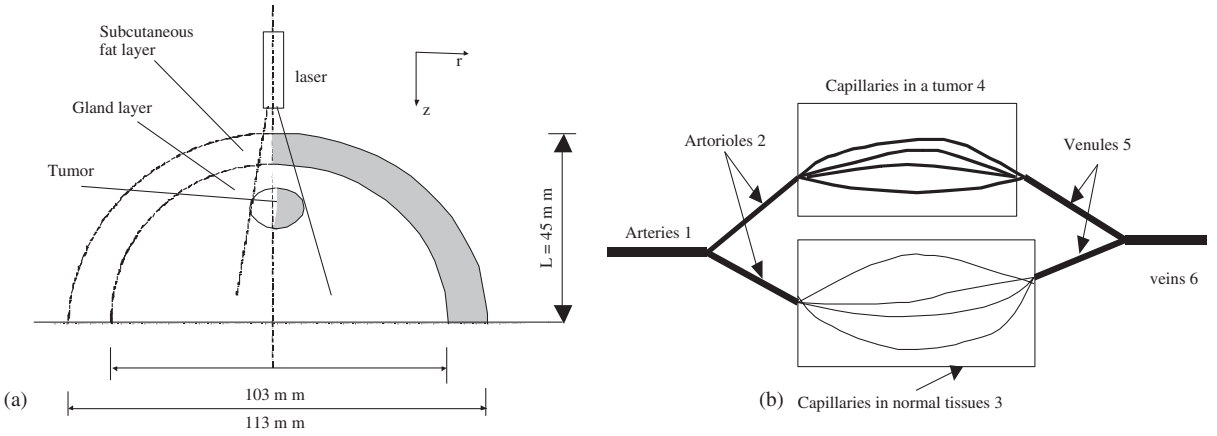

Fig. 1. (a) The schematic of a laser-irradiated breast tumor and (b) the blood circulation network.

Table 1
Physiological data of the vessels in a human breast tumor

Segment number	Vessels	Length (m)	Proximal diameter (10^{-3} m)	Distal diameter (10^{-3} m)	Number of vessels
1	Lateral thoracic artery and lateral mammary arterial branch	0.1	4	3.6	1
2	Arterioles	0.014	0.02	0.02	1.5×10^5
3	Capillaries	0.0005	0.005	0.005	2.3×10^7
4	Tumor vessels	0.0001	0.01	0.01	5×10^3
5	Venules	0.018	0.03	0.03	9×10^5
6	Internal thoracic vein and lateral thoracic vein	0.1	2	2	1

data of the normal blood vessels, including the length and diameters or the cross-sectional areas of the vessel segments, were based on the MRI image [14] and the available data [15]. Table 1 lists the representative data.

3. Analysis

3.1. Analysis of heat transport in living tissue

The temperature distribution induced by laser irradiation in the target zone and other areas is governed by the bioheat equation [16], which is in the following form:

$$\rho_t c_t \frac{\partial T_t}{\partial t} = \lambda_t \left(\frac{\partial^2 T}{\partial^2 r} + \frac{1}{r}\frac{\partial T}{\partial r} + \frac{\partial^2 T}{\partial^2 z} \right) + Q + \omega \rho_b c_b (T_b - T_t). \tag{1}$$

When the laser beam hits the skin surface, the laser energy is partially absorbed, scattered, and transmitted. The laser power intensity along the tissue depth is expressed by Lambert–Beer's law, as follows:

$$I(r, z) = I_0(r) \mathrm{e}^{-(a+s)z}. \tag{2}$$

Heat generation due to scattering is assumed to be negligible; therefore, the specific absorption rate in the target zone can be expressed as follows:

$$Q = -\frac{\mathrm{d}I}{\mathrm{d}z} = a I_0(r) \mathrm{e}^{-(a+s)z}. \tag{3}$$

Since the diameter of the tumor is 10 mm; the irradiated diameter is set to be 10 mm. For the area not exposed to a laser irradiation, the specific absorption rate is set to be 0.

The heat transport in the tissue is subject to the following boundary conditions:

(a) at the skin surface

$$\lambda \frac{\partial T_t}{\partial n} = h(T_t - T_f). \tag{4}$$

(b) At the axis of the symmetry or the base of the breast

$$r = 0 \quad \text{or} \quad z = L \quad \frac{\partial T}{\partial n} = 0. \tag{5}$$

The bioheat equation is discretized using the finite element method (FEM). The finite element equation is developed using the Galerkin weighted residual method, and the matrix form is expressed as follows:

$$[k^{\mathrm{e}}]\{T^{\mathrm{e}}\} + [c]\left\{\frac{\partial T^{\mathrm{e}}}{\partial t}\right\} - \{I^{\mathrm{e}}\} + \{S^{\mathrm{e}}\} = 0, \tag{6}$$

where

$$[k^{\mathrm{e}}] = \int\int_{\mathrm{e}} \lambda \left(\frac{\partial [N]^{\mathrm{T}}}{\partial r}\frac{\partial [N]}{\partial r} + \frac{\partial [N]^{\mathrm{T}}}{\partial z}\frac{\partial [N]}{\partial z}\right) r \,\mathrm{d}r \,\mathrm{d}z + \int\int_{\mathrm{e}} \omega_{\mathrm{b}}\rho_{\mathrm{b}}c_{\mathrm{b}}[N]^{\mathrm{T}}[N] r \,\mathrm{d}r \,\mathrm{d}z - \int_{\mathrm{s}} h[N]^{\mathrm{T}}[N] r \,\mathrm{d}s,$$

$$[c] = \int\int_{\mathrm{e}} \rho_{\mathrm{t}}c_{\mathrm{t}}[N]^{\mathrm{T}}[N] r \,\mathrm{d}r \,\mathrm{d}z,$$

$$\{I^{\mathrm{e}}\} = aI_0(x)\int\int_{\mathrm{e}} [N]^{\mathrm{T}}\mathrm{e}^{-kz} r \,\mathrm{d}r \,\mathrm{d}z + \omega_{\mathrm{b}}\rho_{\mathrm{b}}c_{\mathrm{b}}T_{\mathrm{b}}\int\int_{\mathrm{e}} [N]^{\mathrm{T}} r \,\mathrm{d}r \,\mathrm{d}z,$$

$$\{S^{\mathrm{e}}\} = \int_{\mathrm{s}} hT_{\mathrm{f}}[N]^{\mathrm{T}} r \,\mathrm{d}s. \tag{7}$$

The global equation system is then formed from these finite element equations. A forward difference approximation to the time derivative and the conjugate gradient (CG) method are used in order to compute the algebraic equations of temperature.

3.2. Analysis of blood flow in the human breast

The blood flow in the breast is expressed by one-dimensional non-linear equations of pulsatile flow in an elastic tube. The continuity and momentum equation may be, respectively, defined as

$$\frac{\partial A}{\partial t} + \frac{\partial q}{\partial x} = 0, \tag{8}$$

$$\frac{\partial q}{\partial t} + \frac{\partial}{\partial x}\left(\frac{q^2}{A}\right) + \frac{A}{\rho}\frac{\partial P}{\partial x} = -\frac{2\pi v r}{\delta}\frac{q}{A}. \tag{9}$$

The tube law in the arteries is expressed as in [17].

$$P(x,t) - P_0 = \frac{4}{3}\frac{Eh}{r_0}\left(1 - \sqrt{\frac{A_0}{A}}\right). \tag{10}$$

In the above equation, E is Young's modulus, h is the wall thickness, and r_0 is the radius of the vessels. The tube law in the microcirculation and veins can be expressed as in [18]

$$p - p_0 = k_p \left[1 - \left(\frac{A}{A_0} \right)^{-3/2} \right], \tag{11}$$

where k_p is the coefficient proportional to the stiffness of the tube wall and A_0 is the cross-sectional area in the initial state. The temperature of blood flow in the vessels is given as in [19].

$$\frac{\partial T_b}{\partial t} + \frac{q}{A}\frac{\partial T_b}{\partial x} = -\omega T_b - \frac{h_{ves} A_s}{\rho_b c_b A}(T_b - T_t). \tag{12}$$

The system equations (Eqs. (8)–(11)) are solved by applying the boundary conditions at the inlet, outlet, and the bifurcation. A physiological pulsatile flow is assumed at the inlet [20].

$$\begin{aligned} q_{in} &= q_{max}(0.251 + 0.290(\cos \Phi + 0.97 \cos 2\Phi + 0.47 \cos 3\Phi + 0.14 \cos 4\Phi)), \\ \Phi &= \omega_{rd} t - \sqrt{\frac{\omega_{rd}}{\pi}}. \end{aligned} \tag{13}$$

Since there is no pulsation of pressure in the veins, the outlet pressure is assumed to be 5 mmHg, which remains constant. At the bifurcations, the pressure is assumed to be continuous and the inflow and outflow are balanced. The inlet blood temperature is assumed to be 37 °C.

The two-step Lax–Wendroff method was used to transform the system of partial differential equations (8)–(11) into algebraic equations. The energy equation (12) may be solved after obtaining the blood flow rate and cross-sectional area from Eqs. (8)–(11). A detailed description of the computational method can be obtained from [19].

3.3. Analysis of oxygen distribution in blood vessels and tissue

The classical Krogh cylinder approach [10] was used to analyze the oxygen distribution in a tissue. In the Krogh model, it is assumed that the tissue can be subdivided into parallel and evenly spaced cylindrical tissue units, and that each of the units has a capillary which supplies oxygen to the tissue region surrounding it. Thus, a normal and tumor tissue unit were extracted in order to analyze the oxygen distribution in the vessels and the tissue. The schematic of the computed domain is shown in Fig. 2. The equation governing oxygen transport in the vessels and the tissue can be expressed as follows:

$$\alpha \frac{\partial PO_2}{\partial t} + u\alpha \frac{\partial PO_2}{\partial x} = D\alpha \left(\frac{\partial^2 PO_2}{\partial x^2} + \frac{\partial^2 PO_2}{\partial y^2} \right) - M, \tag{14}$$

where PO_2 is the partial pressure of oxygen, α is the oxygen solubility, D is the oxygen diffusivity, and M is the oxygen consumption rate. At present, the oxygen consumption rate is considered to exhibit zero-order kinetics, that is

$$\begin{aligned} &M = M_0 = const \quad \text{for } PO_2 > 0, \\ &M = 0 \quad \text{for } PO_2 = 0. \end{aligned} \tag{15}$$

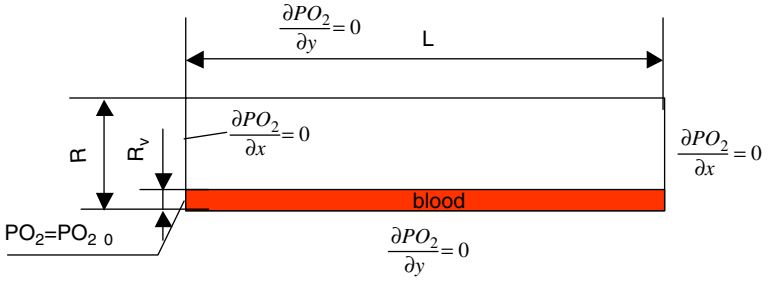

Fig. 2. The Krogh cyliner model for the normal and tumor tissue units. (1) Normal tissue unit: $R_v=3\,\mu m$, $R=30\,\mu m$, $L=500\,\mu m$, (2) Tumor tissue unit: $R_v=6\,\mu m$, $R=60\,\mu m$, $L=100\,\mu m$.

The following boundary conditions are supplemented in Eq. (14):

$$\begin{aligned} &x=0,\ r\leqslant R_{\mathrm{v}}, \quad \mathrm{PO_2}=\mathrm{PO_{20}},\\ &x=0,\ R_{\mathrm{v}}\leqslant r\leqslant R \quad \text{or} \quad x=L,\ R_{\mathrm{v}}\leqslant r\leqslant R \quad \frac{\partial \mathrm{PO_2}}{\partial x}=0,\\ &r=0 \quad \text{or} \quad r=R \quad \frac{\partial \mathrm{PO_2}}{\partial r}=0. \end{aligned} \tag{16}$$

With respect to the transformation of the oxygen convective-diffusion equation, a simple explicit scheme, similar to that of energy equation (12), was used.

3.4. Coupling method of the analysis models

In order to solve the above-mentioned hyperthermia-tissue–blood flow interaction problem formulated above, the weak coupling method was employed.

Fig. 3 shows the schematic of the data transfer between these models. First, the blood pressure and the flow rate in different vessels are computed through the blood circulation model of the breast. The blood perfusion rate within one heart beat in the normal and tumor tissues thus obtained is transferred to the FE thermal model. Second, the temperature in the normal and tumor tissues under laser irradiation is computed by the FE thermal model and the average tumor temperature is transferred to the blood circulation model. It has been observed that heating a tumor at 41–42 °C for a duration can induce an approximately two-fold increase in the tumor blood flow [13]. Therefore, the response of the blood vessels to the tumor temperature is assumed to be

$$A=A_0 e^{b(T-T_0)}, \tag{17}$$

where A_0 and T_0 are the cross-sectional area and blood temperature before heating, respectively, and b is the variation coefficient. Based on the experimental results, the value of b may be expressed as follows:

$$\begin{aligned} &b=0.1 \quad T=39\text{–}42\,^{\circ}\mathrm{C},\\ &b=-0.1 \quad T>42\,^{\circ}\mathrm{C}. \end{aligned} \tag{18}$$

Since the cross-sectional area of the blood vessels in the heating area under different tumor average temperatures is computable according to Eq. (17), the new blood perfusion due to a change in the blood

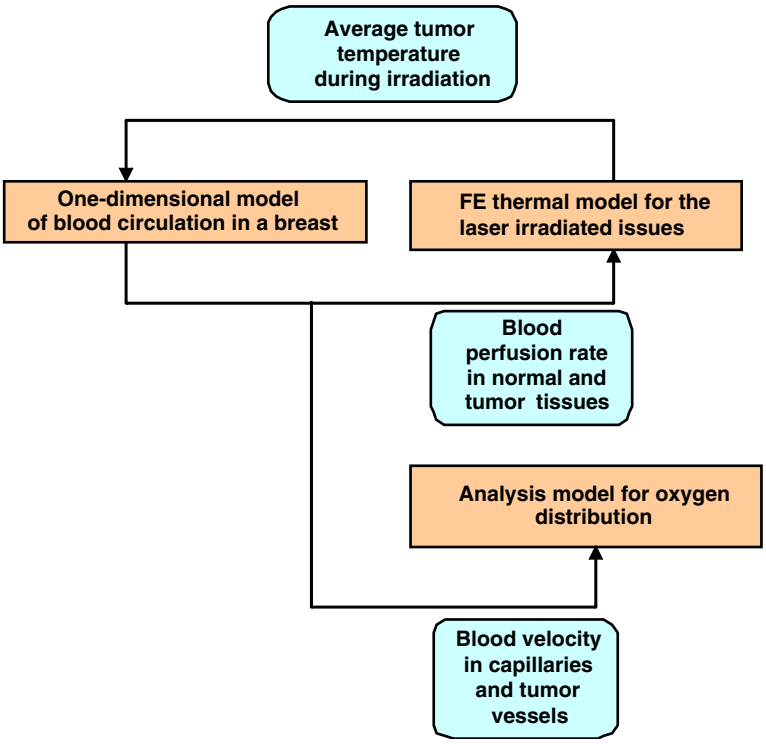

Fig. 3. The method of data transfer between the analysis models.

vessel dimensions can be obtained by the one-dimensional blood circulation model and may be transferred to the FE model instead of the old values. Simultaneously, the new blood velocities are input to the oxygen analysis model for the computation of oxygen partial pressure in the normal and tumor tissue units.

3.5. Physical and physiological parameters

Three sets of parameters are required for calculating the variation of temperature, blood flow, and oxygen distribution in a tumor field. These include (a) thermophysical parameters for the thermal model, (b) parameters related to blood perfusion, and (c) parameters for oxygen distribution. The thermophysical parameters are compiled from data provided by Shih et al. [8], Ng and Sudharsan [11], Shitzer et al. [21], and Diller [22]. The absorption coefficient for the tissue is obtained from Tajima [23]. The heat transfer coefficient at the surface of the breast is calculated by a standard heat transfer correlation for spheres, which is 458 W/m^2K when the temperature of cooling water is 10 °C. Table 2 lists the thermophysical property values used in the analysis.

Using the data provided by Sheng et al. [15], the number of arterioles, capillaries, and venules is 1.5×10^5, 2.3×10^7, and 9×10^5, respectively. Since only a limited amount of data are available regarding tumor vessel density, we deduced the tumor vessel number from the observed average tumor blood flow rate. Ng and Sudharsan [11] suggest that the blood perfusion in the breast tumor changes from 8 to 80 ml/100 g/min. Thus, we can deduce the number of tumor vessels from the blood perfusion rate,

Table 2
Thermal physical property values used in the numerical computation

	Density (kg/m^3)	Specific heat (kJ/kg K)	Thermal conductivity (W/m)	Viscosity (m^2/s)	Absorption coefficient (m^{-1})
Subcutaneous fat	930	2.77	0.22		100
Gland	1050	3.77	0.48		100
Tumor	1050	3.77	0.48		100
Blood	1100	3.30	0.45	4×10^{-6}	

the volume of solid tissue, and the blood flow in a single vessel. In this study, the number of tumor vessels is computed to be approximately 5000.

The effective diffusion coefficient and the oxygen solubility are assumed to be $D=1.5\times10^{-5}\ cm^2/s$ and $\alpha = 3 \times 10^{-5}\ cm^3\ O_2/cm^3/mmHg$, respectively. The metabolic rate of oxygen consumption is assumed to be $3.3 \times 10^{-5}\ cm^3\ O_2/cm^3/s$ [24].

4. Results

In this study, two situations under a laser irradiation of $1.3\ W/cm^2$ were considered. In the first situation, the blood is well perfused in the peripheral part of the tumor, whereas in the other situation, the blood is well perfused in the central core of the tumor.

Fig. 4(a) shows the finite-element grid network of the computed model. The tumor and gland tissues differ in terms of blood perfusion, i.e., the blood perfusion is higher in the tumor tissue. The temperature distribution at different times under the laser irradiation is shown in Fig. 4(b). As seen in this figure, the laser energy is transferred deeply into the tissue with time, and the average temperature within the irradiated tumor increases.

The variations of the average tumor temperature and the tumor blood perfusion are plotted in Fig. 5(a) and (b), respectively. Since the modification of the tumor blood flow induced by the heating treatment depends not only on the therapeutic temperature but also on the heating duration, it is assumed that the variation of the vessels due to the heating treatment occurs 5 min after the heating. Fig. 5(a) shows the average tumor temperature profile for a heating duration of 1200 s. It is observed that the temperature in the tumor without vessels displays the most rapid increase, the temperature in the tumor wherein blood is well perfused in the core displays a lesser increase, while that in the tumor well perfused in the peripheral part displays the least increase. The difference between the highest and the lowest temperatures is 0.6 °C. The variation of the tumor blood perfusion during heating is plotted in Fig. 5(b). In the coupling computing, we addressed the time delay in the variation of the blood perfusion as follows: the blood perfusion variation pattern remains the same within 5 min of heating during the temperature distribution computation; subsequently the computation of the blood flow will be started with a new average tumor temperature. Thus, the blood perfusion within a period of 1 s in Fig. 5(b) corresponds to the blood perfusion within 5 min of heating in Fig. 5(a). Four different types of blood perfusions are observed within 1200 s of heating. Furthermore, it is found that when the tumor has a well-perfused periphery, the blood perfusion rate can be increased for longer durations under laser irradiation, but the tumor temperature in this case is not as easily enhanced as in the case of a tumor with a well-perfused core.

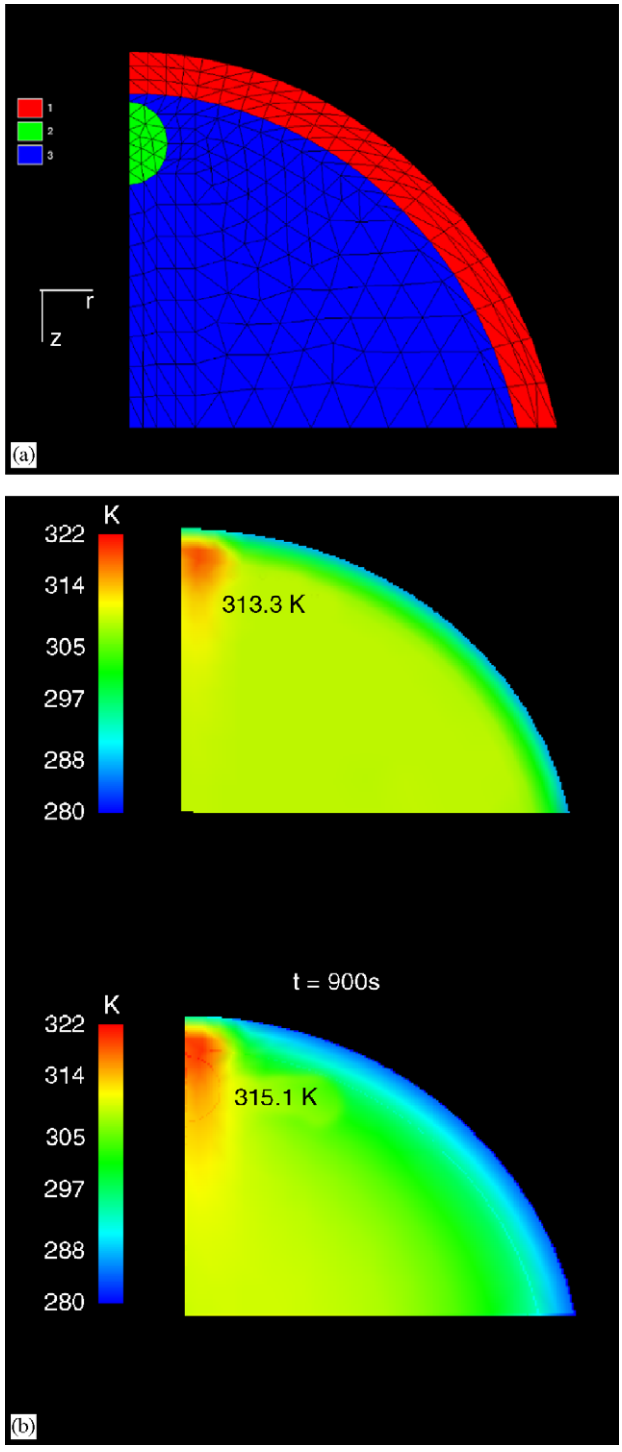

Fig. 4. (a) FEM mesh network of the computational domain and (b) temperature distribution in the human breast under laser irradiation (Laser Power: 1.3 W/cm^2).

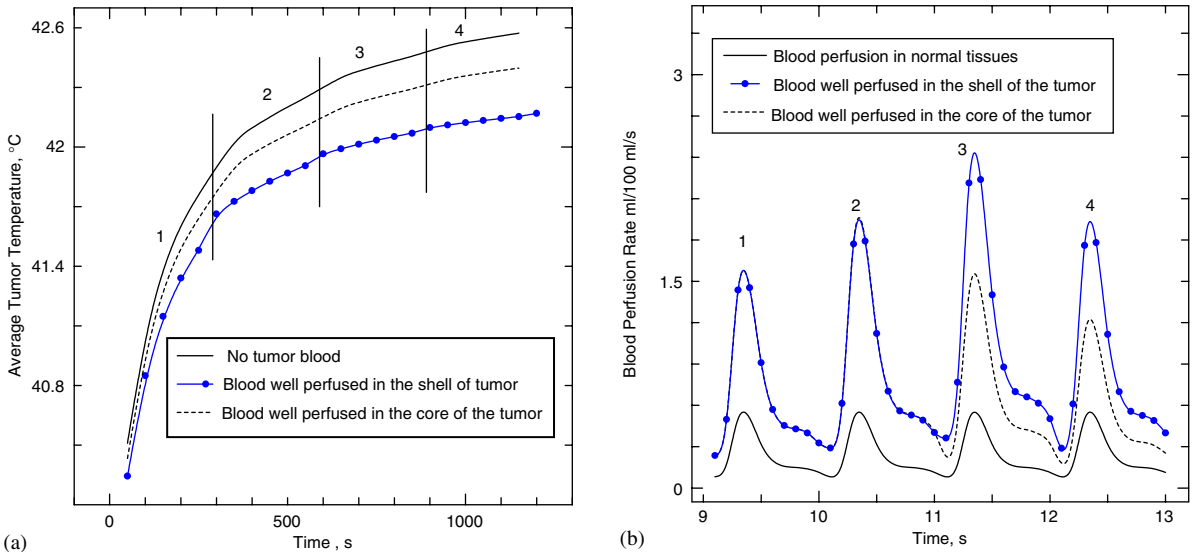

Fig. 5. Variation of (a) Average tumor temperature and (b) tumor blood perfusion under laser irradiation.

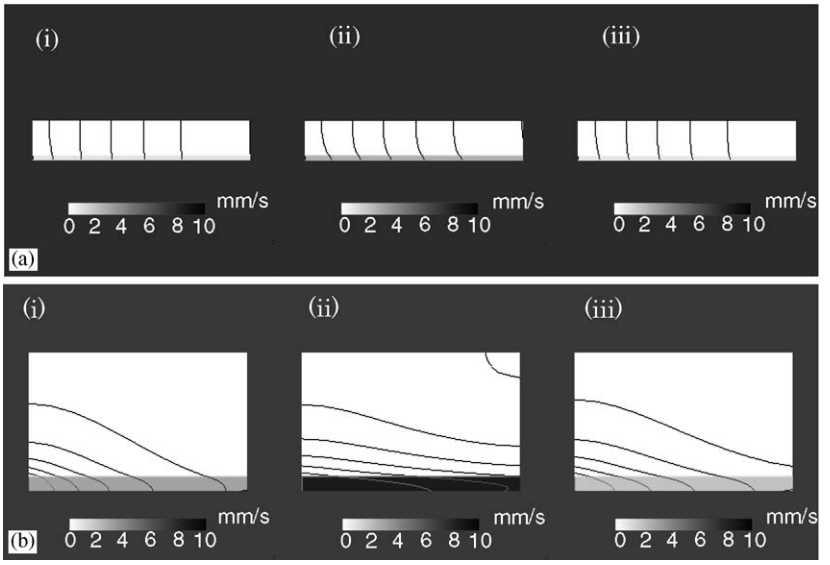

Fig. 6. Oxygen distribution in the normal (a) and tumor (b) tissue units within a period.

Fig. 6(a) shows the distribution of PO_2 in the normal tissue unit during a period. PO_2 in the inlet of a capillary is assumed to be 50 mmHg, and the pulsatile capillary blood velocity from the one-dimensional model is assigned to the vessel inlets. The tissue volume has a diameter of 60 μm and a length of 0.5 mm, and the capillary inside the tissue volume has a diameter of 6 μm. Due to the small diameter of the vessels and the low flow rate, the difference in the PO_2 levels in vessels and the tissue is less, and the spatial and

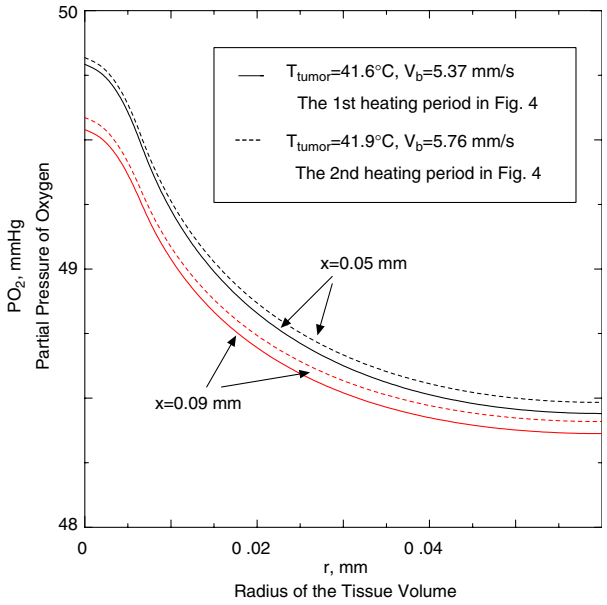

Fig. 7. Distribution of the tumor partial pressure of oxygen for different blood perfusion.

temporal distribution is almost uniform. The PO_2 distribution in the tumor tissue during a period is shown in Fig. 6(b). The tumor tissue volume has a diameter of 120 μm and a length of 0.1 mm. The tumor blood vessel is 12 μm in diameter. The PO_2 distribution in the tumor tissue volume appears different from that in the normal tissue volume. The PO_2 gradient in the tumor vessel and the tissue is larger in comparison with that in the normal tissue; thus, the region that is away from the tumor vessel has a lower PO_2 than that near the tumor vessel, and the distribution is inclined to become heterogeneous.

The variation of PO_2 with different blood velocities in the tumor tissue unit is shown in Fig. 7. The solid lines represent the distribution profiles with a lower blood velocity in the initial heating period, and the dotted lines represent the distribution profiles in the later heating period at a higher blood velocity. Since the variation of blood velocity is caused by heating, we can thus obtain the variation of PO_2 at different temperature levels.

5. Discussion

Improving the efficiency of tumor treatments has always been a significant concern. In this study, a coupling numerical model is presented for the study of the tumor blood perfusion and the distribution of PO_2 under laser irradiation. The model includes the blood flow rate, temperature distribution, and PO_2 distribution inside the vessels and the tissue unit. This model can be used to quantify the interaction of hyperthermia, blood flow, and oxygen distribution. The characteristic feature of this coupling model is to couple the heat and mass diffusion model with a systemic flow model for the determination of blood flow prescribed for the heat and mass diffusion model.

Our model has several limitations. First, lumped parameters that are representative of different vessels are required; these parameters are largely dependent on the experiment. Second, it only models the geometric differences between normal and tumor vessels. The tumor vasculature, although similar to the normal vessels in several aspects, has its own characteristic features. The difference in the vessel wall permeability may also be included. In addition, the heat transfer between the larger arteries in the breast and the tissue are not considered. Studies have shown that the thermal effect of larger arteries cannot be neglected [7,8,25]. Due to the limitations of the two-dimensional model, the larger arteries in the breast are treated as the same media as that surrounding them.

6. Summary

In conclusion, the proposed coupling model can be used to investigate hyperthermia-blood flow-oxygen distribution interaction. The initial results show that for the tumors with different blood perfusion distribution, the variation of tumor temperature after heating is different. Accordingly, the tumor blood perfusion displays a different modification tendency. Moreover, the oxygen distribution gradient is greater in the tumor tissue than in the normal tissue, particularly near the tumor vessels.

The coupling model presented here provides a tool to analyze the relationship between blood flow, vessel temperature, and oxygen distribution. The ultimate goal of this study is to monitor the spatial and temporal variation of the tumor blood perfusion and its effect on the oxygen distribution in the treatment of cancer. The future extension of this research would be the study of the blood perfusion and oxygen distribution in differently shaped tumors with different heating sources.

References

[1] B. Edirich, F. Hammersen, K. Messmer, Hyperthermia-induced changes in tumor microcirculation, in: R.D. Issels, W. Wilmanns (Eds.), Application of Hyperthermia in the Treatment of Cancer, Springer, Berlin, 1988, pp. 45–59.

[2] D. Akyürekli, L.H. Gerig, G.P. Raaphoost, Changes in muscle blood flow distribution during hyperthermia, Int. J. Hyperthermia 13 (1997) 481–486.

[3] A. Shakil, J.L. Osborn, C.W. Song, Changes in oxygenation status and blood flow in a rat tumor model by mild temperature hyperthermia, Int. J. Radiat. Oncol. Biol. Phys. 43 (1999) 859–865.

[4] R.J. Griffin, A. Ogawa, C.W. Song, A novel drug to reduce tumor perfusion: antitumor effect alone and with hyperthermia, Radiat. Res. 154 (2000) 202–207.

[5] Z.P. Shulman, B.M. Khusid, I.V. Fain, Effect of blood perfusion variation on heat transfer under local hyperthermia treatment, Appl. Mech. Eng. 2 (1997) 89–106.

[6] C. Guiot, E. Madon, D. Allegro, P.G. Piantà, B. Biotto, P. Gabriele, Perfusion and thermal field during hyperthermia, experimental measurements and modeling in recurrent breast cancer, Phys. Med. Biol. 43 (1998) 2831–2843.

[7] M.C. Kolios, M.D. Sherar, J.W. Hunt, Large blood vessel cooling in heated tissues: a numerical study, Phys. Med. Biol. 40 (1995) 477–494.

[8] T.C. Shih, H.S. Kou, W.L. Lin, The impact of thermally significant blood vessels in perfused tumor tissue on thermal dose distributions during thermal therapies, Int. Commun. Heat Mass Transfer 30 (7) (2003) 975–985.

[9] R.K. Jain, Determinants of tumor blood flow: a review, Cancer Res. 48 (1988) 2641–2658.

[10] A. Krogh, The number and distribution of capillaries in muscles with calculations of the oxygen pressure head necessary for supplying the tissue, J. Physiol. (London) 52 (1919) 409–515.

[11] E.Y.K. Ng, N.M. Sudharsan, An improved three-dimensional direct numerical modeling and thermal analysis of a female breast with tumor, Proceedings of the Institute of Mechanical Engineers, Part H, J. Eng. Med. 215 (H1) (2001) 25–37.

[12] J.R. Less, T.C. Skalak, E.M. Sevick, R.K. Jain, Microvascular architecture in a mammary carcinorma: branching patterns and vessel diameters, Cancer Res. 51 (1991) 265–273.
[13] C.W. Song, Modification of blood flow, in: M. Molls, P. Vaupel (Eds.), Blood Perfusion and Microenvironment of Human Tumors, Springer, Berlin, 2000, pp. 193–217.
[14] K. Hiramatsu, M. Matsuyama, New Anatomic Atlas for Image Diagnosis-4, Medical View, third ed., 1999, pp. 80–81 (in Japanese).
[15] C. Sheng, S.N. Sarwal, K.C. Watts, A.E. Marble, Computational simulation of blood flow in human systemic circulation incorporating an external force field, Med. Biol. Eng. Comput. 33 (1995) 8–17.
[16] H.H. Pennes, Analysis of tissue and arterial blood temperatures in the resting human forearm, J. Appl. Physiol. 1 (2) (1948) 93–122.
[17] M.S. Olufsen, C.S. Peskin, W.Y. Kim, E.R. Pedersen, A. Nadim, J. Larsen, Numerical simulation and experimental validation of blood flow in arteries with structured-tree outflow conditions, Ann. Biomed. Eng. 28 (2000) 1281–1299.
[18] A.H. Shapiro, Steady flow in collapsible tubes, Trans. ASME, J. Biomech. Eng. 99 (1977) 126–147.
[19] Y. He, H. Liu, R. Himeno, A one-dimensional thermo-fluid model of blood circulation in the human upper limb, Int. J. Heat Mass Transfer 47 (2004) 2735–2745.
[20] H. Liu, T. Yamaguchi, Waveform dependence of pulsatile flow in a stenosed channel, Trans. ASME J. Biomech. Eng. 123 (2001) 88–96.
[21] A. Shitzer, L.A. Stroschein, P. Vital, R.R. Gonzalez, K.B. Pandolf, Numerical analysis of an extremity in a cold environment including counter current arterio-venous heat exchange, Trans. ASME, J. Biomech. Eng. 119 (1997) 179–186.
[22] K.R. Diller, Modeling of bioheat transfer processes at high and low temperatures, in: Y.I. Cho (Ed.), Advances in Heat Transfer, vol. 22, Academic Press, New York, 1992, p. 302.
[23] K. Tajima, Thermal analysis of medical treatment using laser irradiation, Graduation Thesis of The University of Tokyo, 1995.
[24] R. Hsu, T.W. Secomb, A Green's function method for analysis of oxygen delivery to tissue by microvessel networks, Math. Biosci. 96 (1989) 61–78.
[25] Y. He, H. Liu, R. Himeno, M. Shirazaki, Numerical and experimental study of the effect of blood circulation on the human finger temperature, Trans. JSME (B) 71 (2005) 641–648 (in Japanese).

Y. He received her B.E. (1989) and M.E. (1992) degrees from Dalian University of Technology, China, and her D.E. degree (1999) from The University of Tokyo, Japan. She works as a research assistant at the Computational Biomechanics Unit, RIKEN. Her research interests include numerical and experimental studies of blood flow and heat transfer in living tissues.

M. Shirazaki received his B.E. (1992) and M.E. (1994) degrees from Hokkaido University, and his D.E. degree (1999) from The University of Tokyo, Japan. He is an associate professor of the Course of Multimedia Studies in Yokohama National University. His current research interests are fluid-structure interaction including heat transfer and large–scale parallel computing.

H. Liu received his B.S. degree (1985) from Dalian University of Technology, China, and completed his M.S.E. (1989) and Ph.D. (1992) from Yokohama National University, Japan. He is a professor at the Department of Electronics and Mechanical Engineering in Chiba University. His research interests focus on computational fluid dynamics, biological fluid dynamics, physiological fluid dynamics, and image-based modeling of cardiovascular arterial vessels.

R. Himeno received his B.E. (1977) and M.E. (1979) degrees from Kyoto University and received his D.E. degree (1989) from The University of Tokyo. He is the unit leader of the Computational Biomechanics Unit and the director of the Advanced Center for Computing and Communication, RIKEN. His current interests include computational biomechanics simulation and structure–fluid coupled simulation.

Z.G. Sun received his B.E. (1985) from Tianjin University, China, M.E. (1988) from Jilin University of Technology, China, and D.E. (1997) degrees from Gifu University, Japan. He is a senior researcher at Advanced Simulation Technology of Mechanics Co., Ltd., RIKEN. His current interests include computational biomechanics and nonlinear FEM numerical simulation.